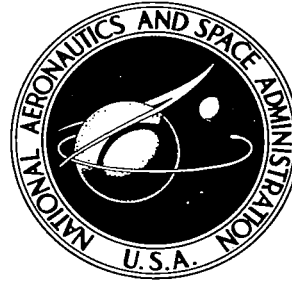


# NASA TECHNICAL REPORT

NASA TR R-197



NASA TR R-197

0.1

LOAN COPY: R  
AFWL (W  
KIRTLAND AFB

0068071



## SUMMARY OF ROLL CONTROLS APPLICABLE TO FIN-STABILIZED VEHICLES

*by Eugene D. Schult*

*Langley Research Center*

*Langley Station, Hampton, Va.*



0068071

SUMMARY OF ROLL CONTROLS APPLICABLE  
TO FIN-STABILIZED VEHICLES

By Eugene D. Schult

Langley Research Center  
Langley Station, Hampton, Va.

NATIONAL AERONAUTICS AND SPACE ADMINISTRATION

---

For sale by the Office of Technical Services, Department of Commerce,  
Washington, D.C. 20230 -- Price \$0.50



## SUMMARY OF ROLL CONTROLS APPLICABLE

### TO FIN-STABILIZED VEHICLES<sup>1</sup>

By Eugene D. Schult

#### SUMMARY

This paper discusses the rolling effectiveness of deflected fins, flaps, spoilers, and jet devices which may be employed on fin-stabilized vehicles. The possible applications and some of the significant factors affecting the performance of each device are described. The experimental information has been published previously and was obtained chiefly from free-flight tests of fin-stabilized vehicles at Mach numbers up to approximately 2.0. Comparisons are made in some cases with existing theory, which is also relied upon to indicate trends where data are not available.

#### INTRODUCTION

The National Aeronautics and Space Administration has devoted a part of its research program to the problem of controlling slender, high-speed vehicle configurations. A portion of this program which may be of interest to designers of fin-stabilized vehicles is the study of the effectiveness of various control devices attached to the fins or body of a model to introduce roll in the flight path. The purpose of the present paper is to discuss possible applications of deflected fins, flaps, spoilers, and air jets and to review briefly some of the significant factors that affect their performance. Theory is heavily relied upon to indicate trends where experimental data are not available. Because of the vast amount of effort which has been devoted to the problem of controls, this paper can illustrate only a few highlights. For more complete information, the reader is referred to the bibliography of reference 1 and to references 2 to 51.

#### SYMBOLS

A	aspect ratio, $b^2/s_1$
b	fin span, ft

---

<sup>1</sup>Supersedes declassified NACA Research Memorandum L57A04 by Eugene D. Schult, 1957.

$C_{lp}$	roll damping-moment coefficient per radian of helix angle
$C_{l\delta}$	rolling-moment coefficient per degree of control deflection
$c$	fin chord in streamwise plane, ft
$c_c$	control chord in streamwise plane, ft
$c_r$	fin root chord at fuselage juncture, ft
$d$	body diameter, ft
$h$	projected height of spoiler above fin surface, ft
$I$	polar mass moment of inertia of model, slug-ft <sup>2</sup>
$k$	exponential constant, sec <sup>-1</sup>
$M$	Mach number
$M_{X,c}$	rolling moment due to control, ft-lb
$M_{X,I}$	negative couple due to model inertia, ft-lb
$M_{X,p}$	negative rolling moment due to damping, ft-lb
$n$	number of fins
$p$	rolling velocity, radians/sec
$\dot{p}$	rolling acceleration, $dp/dr$ , radians/sec <sup>2</sup>
$pb/2V$	fin-tip helix angle, radians
$q$	free-stream dynamic pressure, $\frac{1}{2}\rho V^2$ , lb/sq ft
$S$	planform area of all fins to center line, sq ft
$S_c$	total planform area of all control surfaces to center line, sq ft
$S_l$	planform area of two fins (one plane) to center line, sq ft
$t$	fin thickness, ft
$V$	forward velocity, ft/sec
$x$	longitudinal distance from fin leading edge to spoiler, ft

$\delta$	control-surface deflection measured in streamwise plane, deg
$\rho$	stream density, slugs/cu ft
$\tau$	time, sec
$\tau_s$	steady-state time lag
$\phi$	flap trailing-edge angle measured between upper and lower flap surfaces in the streamwise plane, deg

A prime (') after a symbol indicates that the value has been nondimensionalized by dividing it by the value for  $A = 2$ .

## DISCUSSION

### Statement of the Problem

For simplicity, it is customary when dealing with pure roll of a finned vehicle to express the rolling effectiveness of the control device in terms of the helix angle generated by the fin tips. From the helix angle it is then possible to determine the roll displacement per foot of range.

In order to gain a common understanding of the terms employed, reference is made to figure 1. The control in this case consists of canted fins all equally deflected to obtain pure roll. The resulting moments are given by the following equations:

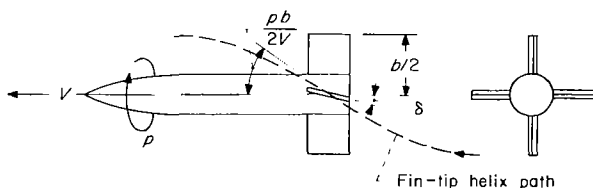


Figure 1.- The finned vehicle in pure roll.

$$M_{X,c} = C_{l\delta} \delta q S b \quad (1)$$

$$-M_{X,p} = C_{lp} \frac{pb}{2V} q S b \quad (2)$$

$$-M_{X,I} = I \dot{p} \quad (3)$$

A summation of these moments set equal to zero yields the usual solutions for both steady-state and transient roll conditions. In steady-state roll ( $\dot{p} = 0$ ), the helix angle per degree of control deflection reduces to the simple expression:

$$\frac{pb/2V}{\delta} = \frac{C_{l\delta}}{-C_{lp}} \quad (4)$$

from which the roll displacement per foot may be obtained by solving for  $p/V$ . Equation (4) shows the helix angle independent of fin scale, whereas the rolling velocity varies inversely with scale. The side effects of altitude or dynamic pressure on the helix angle are not apparent here until the possible fin distortions caused by control or fin air loads are considered. These so-called aeroelastic effects are frequently encountered with flap-type controls and will be examined further when this control is discussed.

Roll-response considerations.- The time lag for the vehicle to reach some design level of roll rate is frequently of interest. In this connection the transient solution given by the following equation illustrates the factors which affect the response history:

$$\left( \frac{pb/2V}{\delta} \right)_{\text{trans}} = \frac{C_{l\delta}}{-C_{lp}} (1 - e^{-k\tau}) \quad (5)$$

where

$$k = -C_{lp} \frac{q}{V} \frac{Sb^2}{2I}$$

and time  $\tau$  is given in seconds. For a given configuration the speed of response is related both to the magnitude of the control input  $C_{l\delta}$  and to the terms in the exponential constant  $k$ . The time to reach some initial level of roll rate is largely a function of the control input since the input determines the initial roll acceleration. On the other hand, the time to reach the final steady-state condition is a function only of  $k$ , which depends on flight conditions and the details of the basic configuration. The present paper will include some effects of changes in configuration on the steady-state time lag.

Types of controls and possible applications.- Of the conventional control types, the deflected fin is still regarded as the simplest and most efficient aerodynamic device for producing roll. Other control arrangements are therefore justified only when necessary to satisfy certain design requirements for particular applications. If these requirements, for example, indicate a need for a fairly constant roll rate over the speed range or for a device which provides roll in but one direction even in a reversed flow of propellant gases, then it appears that certain flap, spoiler, or jet controls would be more suitable than deflected fins.

The experimental data on which the discussion is based were obtained primarily from free-flight tests of fin-stabilized models incorporating these controls. The measurements were made near zero lift and under essentially steady-state roll conditions. The corresponding theoretical estimates of rolling effectiveness were calculated by means of equation (4) from ratios of the calculated coefficients  $C_{l\delta}$  and  $C_{lp}$ . The deflection  $\delta$  is measured in the

streamwise plane, and the control rolling moments are assumed to increase linearly with deflection in accordance with linear theory.

### Deflected Fins

In discussing control by means of fin deflection, an attempt will be made to point out some effects of fin shape and aspect ratio on the steady-state and transient roll performance and to review the influence of fin-fin and fin-body interference.

Effects of planform.- The effect of deflected-fin shape is shown in figure 2, where the steady-state rolling-effectiveness parameter  $\frac{pb/2V}{\delta}$  is plotted against Mach number for several fin arrangements. It is noted that variations

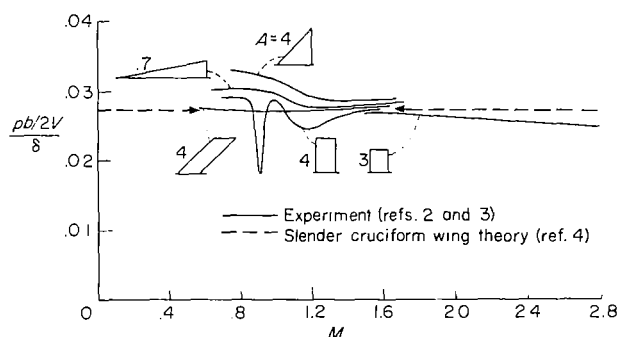


Figure 2.- Rolling effectiveness of deflected fins.

in fin shape for a given aspect ratio are not particularly significant insofar as the steady-state performance is concerned. Sweeping back the rectangular fin produced noticeable improvements by smoothing out the abrupt variations in rolling effectiveness with Mach number. These variations are attributed to the thick, sharp-trailing-edge airfoil sections employed.

### Effects of fin aspect ratio.

Figure 2 also indicates that the steady-state rolling effectiveness is not overly sensitive to differences in aspect ratio for a given type of

planform. This result is in accord with theory, which shows that while the average induced pressures over a deflected fin increase with aspect ratio, both the rolling and damping moments due to these pressures increase in about the same proportion so that their ratio (or steady-state helix angle) remains about the same. (See refs. 4, 5, 6, 20, 21, and 22.)

Probably of greater importance is the influence of aspect ratio on the transient response of the model. It will be recalled in connection with equation (5) that high damping-in-roll coefficients were significant in reducing the time lag to achieve the steady-state roll condition. This is demonstrated more clearly in figure 3, which presents the calculated roll characteristics of a fin-stabilized vehicle as rectangular fins of progressively greater span and aspect ratio are attached. The fin area and deflection remain constant, no interference effects are considered, and the mass of the vehicle is assumed to be concentrated within the body of the model. All characteristics are in the form of ratios relative to the fin on the left. Increasing the aspect ratio from 2 to 10, or by a factor of 5, increased the rolling and damping moments by a factor of approximately 10. The steady-state helix angle remains essentially constant but the roll rate decreases as expected because of the increased span.



The time lag to attain steady-state roll, meanwhile, was reduced by a factor of 10 because of increased damping coefficient and span. If it is desirable to recover the original roll rate with a larger control deflection, then this rate would be reached in one-tenth of the time by using the high-aspect-ratio rather than the low-aspect-ratio fins.

A precautionary comment might be added at this time regarding the method employed to obtain high aspect ratio. For example, in applications where a span increase is not feasible, some improvement in response may be obtained by increasing the fin chord, even though aspect ratio is reduced in the process.

Figure 4 illustrates the result of this design maneuver for rectangular fins of constant span. The Mach number of 1.4

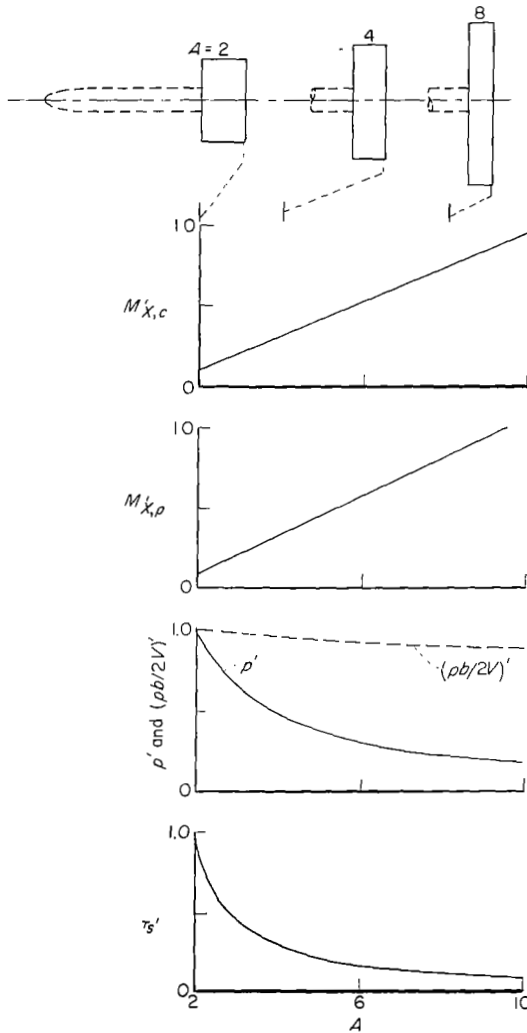


Figure 3.- Estimated effects of fin aspect ratio on roll performance at sea level of a vehicle with four fins of constant area.  $S = 0.444$  sq ft;  $I = 1/20$  slug-ft<sup>2</sup>;  $M = 1.4$ . Theory is from references 5 and 6.

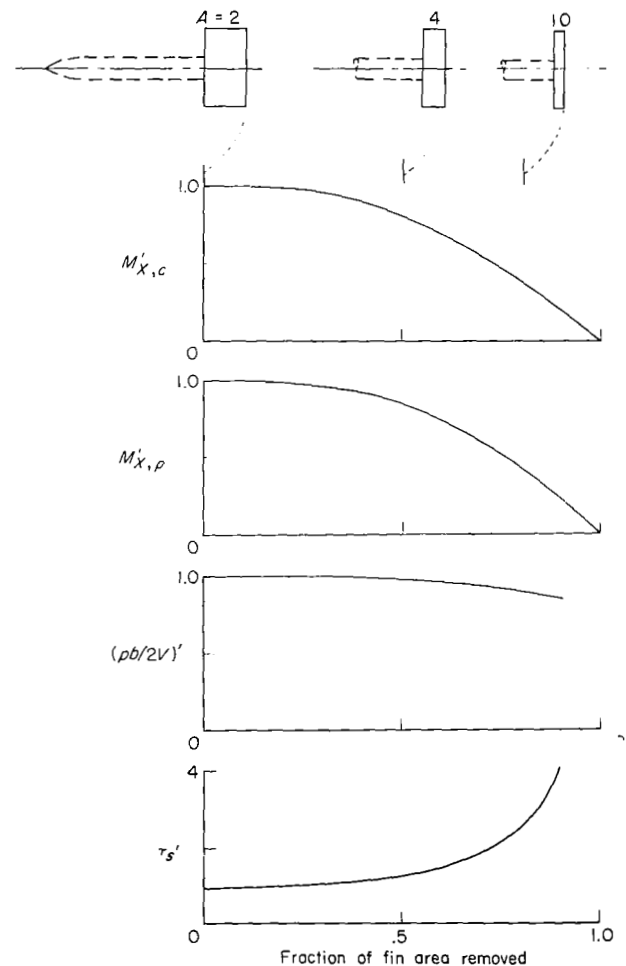


Figure 4.- Estimated effects of fin chord on roll performance at sea level of a vehicle with four fins of constant span.  $b = 2/3$  ft;  $I = 1/20$  slug-ft<sup>2</sup>;  $M = 1.4$ . Theory is from references 5 and 6.

and the basic vehicle are the same as in figure 3. By beginning with a small fin of high aspect ratio and gradually adding more chord (moving from right to left in fig. 4), the response time is improved somewhat. In the process, the reduction in damping coefficient caused by reducing the aspect ratio gradually offsets the benefit of added area until a point is reached where further increases in chord are not justified. Further calculations will show that this "optimum" chord increases with Mach number. Thus, the transient roll performance is significantly improved by employing higher fin aspect ratios if fin area is not sacrificed. On the other hand, increasing the fin area and chord may improve the response even though aspect ratio is reduced in the process. Probably a better alternative to increasing the chord, when span is limited, is to increase the area by adding more fins.

Effects of additional fins.— Some idea of the manner in which more fins affect the roll performance is provided by theory in figure 5. (See refs. 4 and 8.) The variations in moment coefficient and steady-state helix angle with Mach number are calculated for a delta-fin configuration. No body is considered, and the fins are assumed to be of zero thickness. The number of fins is progressively increased from 2 to 4 and then to infinity to illustrate the limiting case. The solid curves apply to  $60^\circ$  delta fins and the dashed curves indicate the trend caused by a slight increase in aspect ratio. Doubling the number of fins does not quite double the moment coefficients, and therefore a progressively smaller gain can be expected with each additional fin until the limiting case is attained. In a practical case the limiting moments are probably less than indicated here and are, no doubt, obtained with fewer fins because of the viscous effects and physical limitations associated with fin thickness which theory does not consider. As the number of fins is increased,

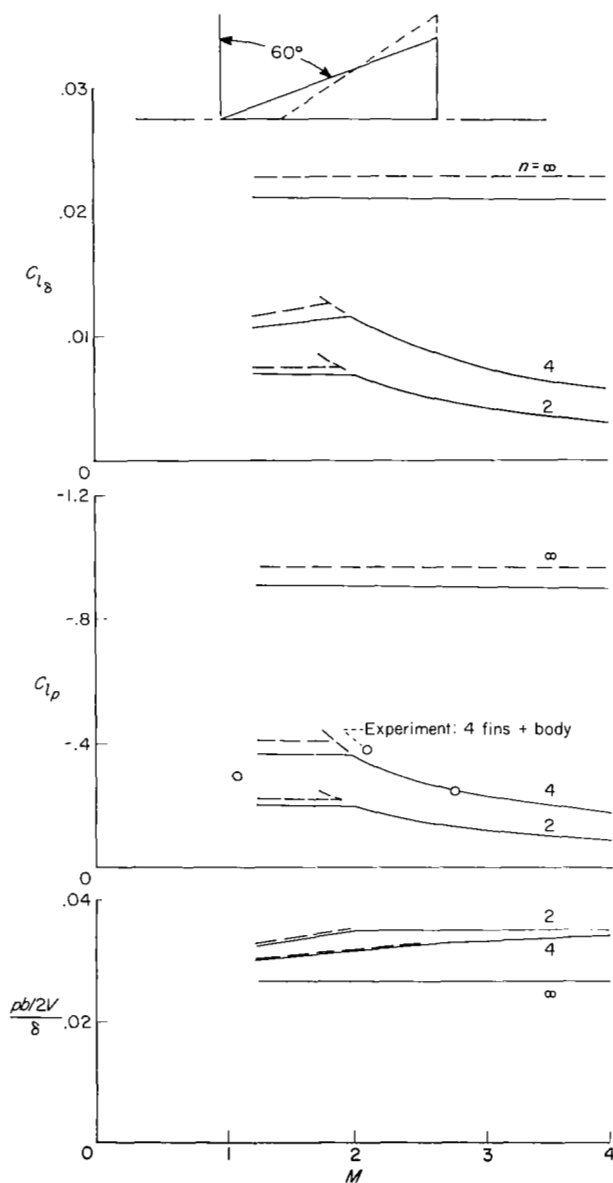


Figure 5.— Estimated effects of increasing number of fins on the rolling moments and effectiveness of deflected fins. No body considered; coefficients are based on area of two fins. Theory is from reference 8 and data are from references 9 and 10.

more gain in the moment coefficients and response can be expected at higher Mach numbers, particularly when fin aspect ratio is also increased. The helix angle is seen to diminish somewhat as more fins are added, and again in the limiting case the level actually obtained is probably lower than predicted for reasons mentioned earlier. Unfortunately the available experimental data, which tend to bear out these predictions, are limited to cases of only 2, 3, or 4 fins. (See refs. 9, 24, and 26.)

#### Effects of body interference.-

After examining the characteristics of isolated fins, it might be appropriate to determine the effect of body interference as the body diameter approaches the total fin span. In figure 6, the reduction factors for the moments and steady-state helix angle of a cruciform configuration are predicted by slender wing-body theory. (See refs. 4, 23, 24, and 25.) These factors are plotted against the ratio of body diameter to fin span and are expressed in terms of the fin-alone characteristics with no body. Notice that the presence of the body has little effect until it covers about a third of the fin span. Above this point the rolling and damping moments of the deflected fins fall off rapidly. The steady-state rolling velocity is least affected by body interference; however, an increase in response time can be expected. If more fins are added, another theory suggests that somewhat larger body diameters might be tolerated before the body effect becomes noticeable. (See ref. 8.) Whether this gain is significant in view of the increased interference between fins is questionable.

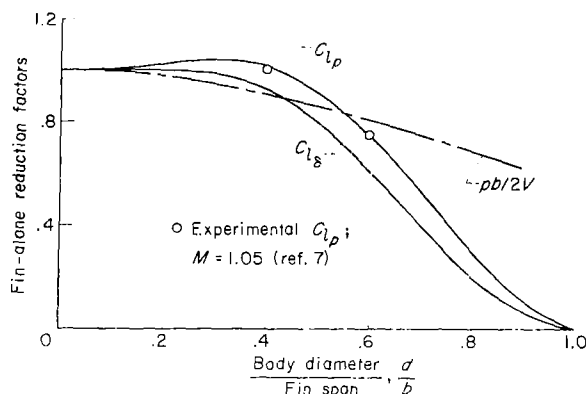


Figure 6.- Effect of body on deflected-fin rolling moments and effectiveness as predicted by slender wing-body theory (ref. 4).

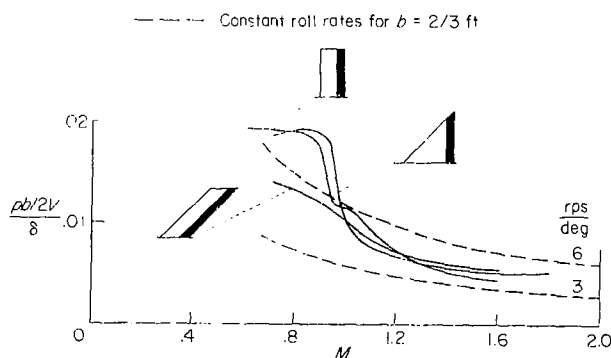


Figure 7.- Effects of fin shape and Mach number on flap rolling effectiveness.  $A = 4$ ;  $S_c/S = 0.2$ ; aluminum fins. Data are from references 11 and 12.

#### Deflected Flaps or Fin Segments

Figure 7 shows the experimental variation of rolling effectiveness with Mach number for a trailing-edge flap of a given area ratio on fins of different shapes. The fin span, aspect ratio, airfoil section, and construction are all essentially constant, and under these conditions the difference in shape is not very significant. Sweeping back the rectangular fin tends to reduce its effectiveness only at subsonic speeds. The tendency of the data to follow

curves of constant roll rate suggests the use of flaps for obtaining a uniform rolling velocity at high speeds.

The primary fin variations which affect flap performance are thickness, section shape, aspect ratio, sweep, and flexibility. The flap variables naturally include span, chord, and deflection. Most of the discussion of fin variations will be centered around full-span flaps of a given size or area ratio and the data will correspond to an equivalent rigid fin in order to divorce the aerodynamic effect of these variations from those caused by structural distortion due to flap loading. The effects of increasing the flap chord and fin flexibility will then be discussed. In all cases, the flap deflection will be defined as the angle in the streamwise plane between the flap mean line and the fin chord plane extended.

Effects of fin thickness and section shape.- At the top of figure 8 some rolling-effectiveness curves are shown for a flap on rectangular fins of different thicknesses and thickness distributions. One trend to be observed is the progressive loss in effectiveness accompanying the increase in airfoil thickness from 3 to 12 percent of the chord. (Compare the solid curves.) The curves for the two 6-percent-thick fins reveal that losses are also caused by variations in flap section shape. One method employed to account for both effects is to relate the flap effectiveness to the flap trailing-edge angle - the angle between the upper and lower surfaces near the trailing edge. (See refs. 2 and 13.) The significance of this angle is demonstrated more clearly in the two plots at the bottom of figure 8. In these plots, samples of data taken at two Mach numbers from tests of a variety of section shapes and thicknesses show the losses in effectiveness due to large trailing-edge angle. At supersonic speeds a good estimate of this loss is provided by the modified linear theory of references 5 and 6. In fact, an extension of this theory to deflected wedge-shaped fins or flaps accounts fairly well for the better performance observed with simple wedge sections than with more conventional shapes. (See refs. 3 and 15.)

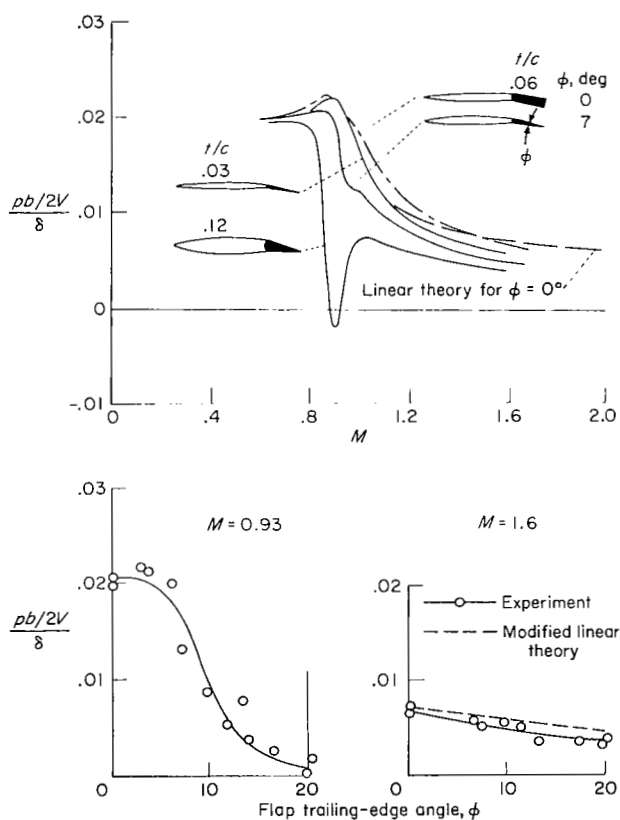
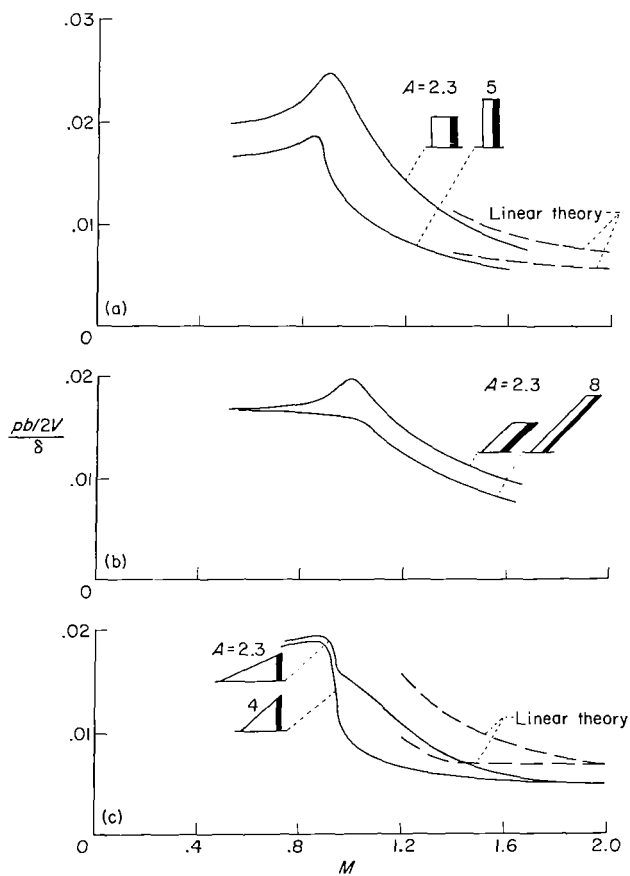


Figure 8.- Effects of fin section thickness and shape on the rolling effectiveness of 0.2-chord flaps on rigid unswept rectangular fins.  $A = 4$ . Theory is from references 5 and 6; data are from references 2 and 13.

Effects of fin aspect ratio and sweep.- For deflected-fin controls, it will be recalled that increasing the aspect ratio increased both the rolling and damping moments in about the same proportion. For flaps, however, theory shows that the rolling moments increase less rapidly with aspect ratio than do the damping moments. (See refs. 5 and 14.) Consequently, the helix angle or ratio of moments tends to decrease as aspect ratio increases. Theory further shows that as the Mach number increases the observed flow becomes more nearly two dimensional so that the effects of aspect ratio become less pronounced. Experimental results in figure 9 illustrate these trends for both the rectangular and triangular fin shapes. In either case it can be seen that increasing the aspect

ratio of the fin reduces the rolling effectiveness, but the differences become less prominent as the Mach number increases. For the rectangular fins, sweepback tends to reduce the effect of aspect ratio on flap effectiveness and to level off the variations in effectiveness with Mach number. (See ref. 2.)

Effects of increasing flap-chord ratio.- The variation of flap effectiveness with flap size is considered next. In figure 10 the fraction of full-chord effectiveness is plotted against the flap chord ratio at two Mach numbers. The experimental points apply to flaps on fins of various shapes. (See refs. 2 and 15.) Two-dimensional or infinite-aspect-ratio theory is indicated by the dashed curves while three-dimensional theory for



(a)  $c_c/c = 0.2$ ;  $\phi = 0^\circ$ ; rigid fin.

(b)  $c_c/c = 0.2$ ;  $\phi = 0^\circ$ ;  $45^\circ$  sweep; rigid fin.

(c)  $S_c/S = 0.2$ ;  $\phi = 7^\circ$ ; aluminum fins.

Figure 9.- Effects of aspect ratio on flap rolling effectiveness. Theory is from references 5, 6, and 14; data are from references 2 and 11.

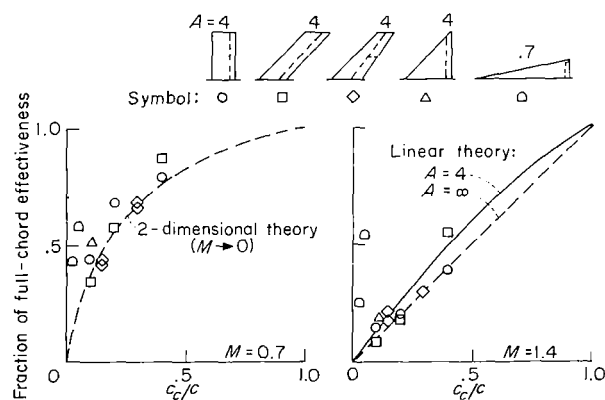


Figure 10.- Fraction of full-chord effectiveness obtained with flaps. Theory is from references 2, 5, 6, and 14; data are from references 2, 11, and 15.

rectangular or triangular fins with an aspect ratio of 4 is shown by the solid curve. At subsonic speeds narrow flaps are quite effective, whereas at supersonic speeds effectiveness is roughly proportional to chord. The two theoretical curves at supersonic speeds are part of a trend which accounts for the relatively high effectiveness at low supersonic speeds of small flaps on fins of very low aspect ratio. This trend becomes less pronounced as the Mach number increases.

**Deflected-tip controls.**- A control obtained by bending up the fin tip is illustrated in figure 11. (See ref. 14.) The theoretical effectiveness of this device, expressed as a fraction of the effectiveness of the conventional deflected fin, is indicated by the curve for all cases in which the fin leading edges are supersonic. The experimental points for two test cases (see ref. 11) are shown by the symbols. The control deflections are again measured in the streamwise plane. Further information on tip controls may be found in references 2, 29, and 30.

**Reversed-flow controls.**- Two other controls of possible interest when reversed flows are encountered are canards and leading-edge flaps. At the top of figure 12 the canards, consisting of small canted surfaces located forward of the main fins, generate a downwash field of sufficient strength over the larger fins to cause negative roll. Since

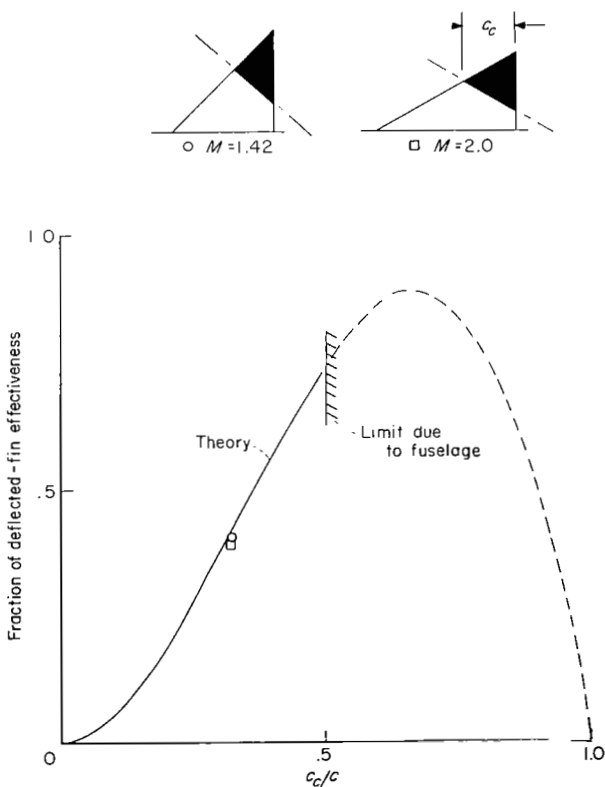
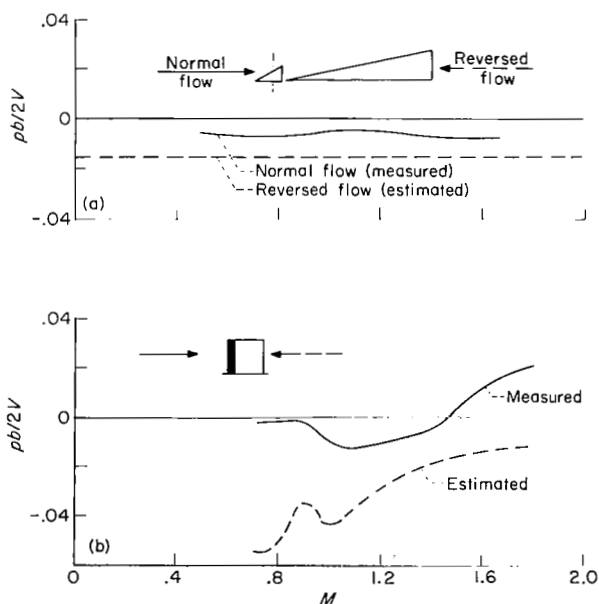


Figure 11.- Relative effectiveness of deflected-tip segments with supersonic leading edges. Theory is from references 6 and 14; data are from references 2 and 11.



(a)  $\delta = 6^\circ$ ;  $S_c/S = 0.05$ .

(b)  $\delta = 5^\circ$ ;  $c_c/c = 0.15$ .

Figure 12.- Canards and leading-edge flaps as reversed-flow controls; references 4, 15, and 28.

surfaces of this type perform in the regular manner in reversed flow, as shown by the estimated curve (refs. 4 and 15), it is possible for them to produce roll in the same direction in either normal or reversed flow. The leading-edge flap in the lower plot also seems promising over a limited Mach number range. (See ref. 28.)

Effects of fin flexibility.- In the preceding discussion of the aerodynamic characteristics of flaps, the associated fins were essentially rigid. It might be of interest to have some idea of the losses in rolling effectiveness due to twisting of the fin by flap loads concentrated along the trailing edge. (See refs. 9, 16, 27, 32, 33, 34, and 35.) In this connection the calculated losses due to flexibility are presented in figure 13 for the case of a trailing-edge flap on an unswept rectangular fin. The results are plotted against Mach number to show the effects of altitude, fin thickness, fin aspect ratio, and fin construction material. As might be expected, the losses at altitude are less because of the lower dynamic pressure  $q$ . A study of the other three plots indicates that with steel fins at least 6 percent thick the losses at sea level over this Mach number range can be kept down to about 3 percent for the aspect-ratio-2 fins and to about 10 percent for the aspect-ratio-4 fins. If sweepback is also incorporated, losses somewhat higher than those shown here may be expected because of the additional fin-bending distortion (ref. 32).

Effects of body shape.- The last point to be discussed in connection with flaps is the possible effect of body shape on rolling effectiveness. Figure 14 shows the results of a test made at zero lift in which the body shape was modified while flap size and body volume were maintained constant. (See ref. 15.) There was no significant change in the steady-state helix angle; however, again the steady-state helix angle is merely a ratio of moment coefficients and gives no indication of the actual effect of body shape on the magnitude of the moments

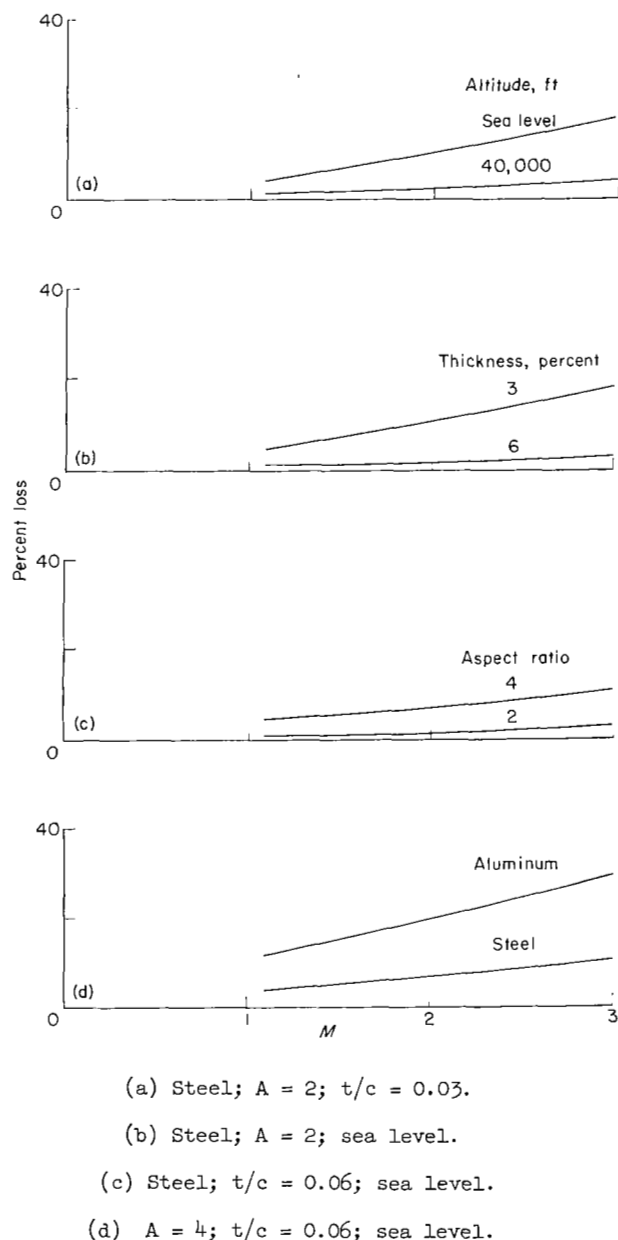


Figure 13.- Losses in rolling effectiveness due to fin flexibility for 0.2-chord trailing-edge flaps on unswept rectangular fins (refs. 6 and 16).

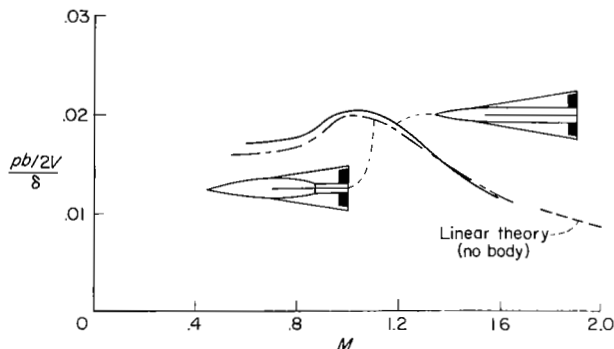


Figure 14.- Effect of a change in body shape on flap rolling effectiveness.  $80^\circ$  delta fins;  $S_c/S \approx 0.10$ . Data are from reference 15; theory is from references 6 and 14.

involved. It might be added that this modification yielded substantial drag reductions.

### Spoiler Controls

At the top of figure 15 is a sketch of a fin-spoiler arrangement which illustrates the approximate loading imposed on the fin by the spoiler and the resultant direction of positive roll.

#### Effects of chordwise location.-

On the basis of this sketch, an improvement in effectiveness might be expected if the spoiler were moved to the rear so that less fin area would be exposed to the negative pressures behind the spoiler. The data presented in the upper plot of figure 15 show some gain through this maneuver, particularly at transonic speeds. Probably more significant is the indication that spoiler locations near the midchord would produce roll in the same direction in reversed flow. This suggests their use in applications where such flows are encountered.

Effects of spoiler height.- One disadvantage of spoilers located forward of the trailing edge is their ineffectiveness at low projections. (See refs. 36, 37, 38, and 42.) In some cases reversals in roll have been reported. An indication of this trend at subsonic speeds is shown by the bottom curve in the center plot of figure 15. This characteristic has been associated with a reattachment of the flow to the fin surface behind the spoiler, which apparently occurs, particularly on thick fins, when the spoiler is lower than a critical height. In reference 37 this critical height has been related to the angle

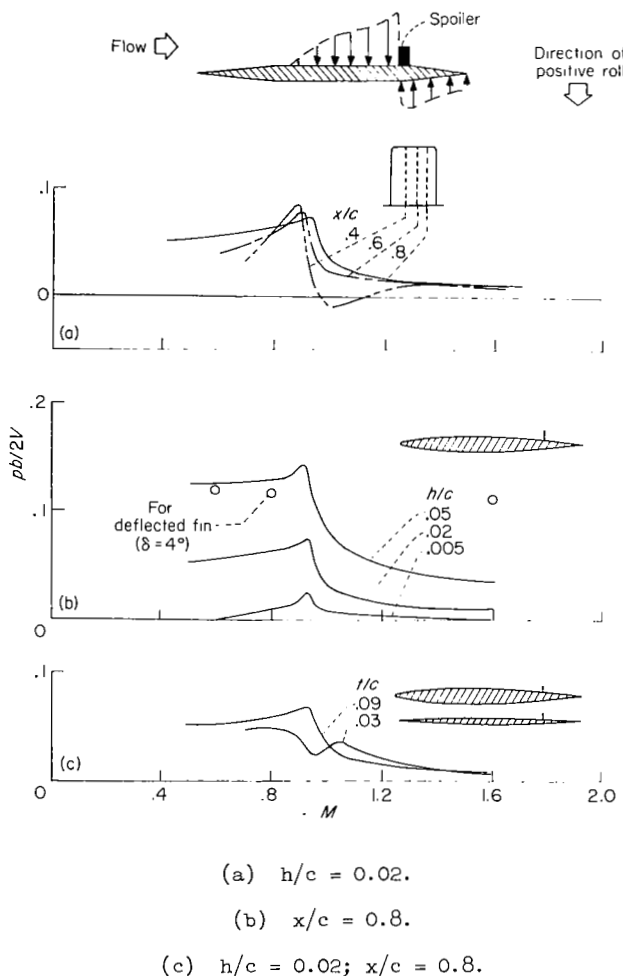


Figure 15.- Spoiler characteristics on unswept rectangular wings (refs. 17, 18, and 19).



between the fin surface and a line connecting the fin trailing edge with the top of the spoiler. Moving the spoiler to the rear or increasing its height generally improved the situation. (See refs. 15, 36, 37, and 42.)

Effects of fin thickness.- In the lower part of figure 15, changes in fin thickness are shown to have little effect for the zero-lift case considered. (See ref. 36.) There is some evidence that spoiler effectiveness is maintained to higher angles of attack on the thicker airfoil sections; this is particularly true at subsonic speeds.

Effects of fin flexibility.- In connection with thin wings which tend to be rather flexible, it has been found that the losses due to flexibility are less with spoilers than with trailing-edge flaps. This might be expected from the sketch at the top of figure 15, which shows a more favorable distribution of loads over the fin than is generally observed with flaps. As a result, the twisting moments and fin distortions are usually small for spoilers. (See ref. 43.)

Effects of spoiler shape.- Some comments on spoiler shapes which tend to reduce the drag penalty are in order. Figure 16 compares the effectiveness of the plain trailing-edge spoiler with that of a ramp having the same height but one-half the incremental drag. (See ref. 15.) The drag of the plain spoiler, incidentally, nearly doubled the drag of the basic cruciform wing-body combination. Locating the plain spoiler forward of the trailing edge caused negative roll, probably for reasons mentioned earlier. This should affect only the roll sense in reverse-flow applications.

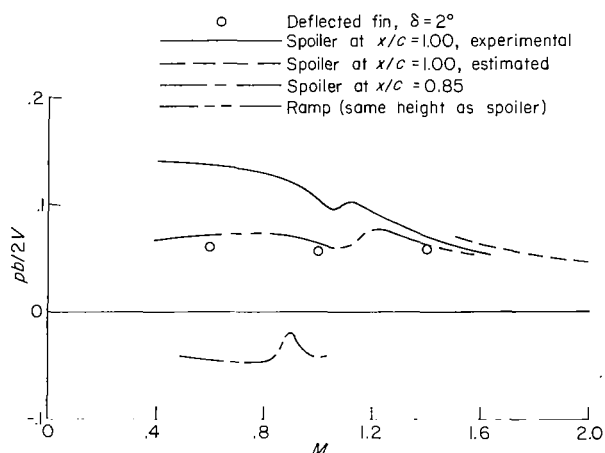


Figure 16.- Spoilers on 80° delta wings;  
 $h/c_r = 0.008$ . See reference 15.

## Air-Jet Devices

The last control to be discussed is the jet device. A number of tests have shown that the total force obtained with jets in combination with fins may exceed the pure reaction force by a substantial margin. (See refs. 44, 45, and 51.)

Effects of chordwise location.- In most cases, the jet control has consisted simply of a number of closely spaced holes drilled in the fin surface and connected by a manifold or duct within the fin to inlets or some external source of air. The jet effectiveness has been found to be roughly proportional to flow rate, and trailing-edge locations seem to be the most satisfactory, although more forward positions are also satisfactory for swept rectangular fins.

#### Effects of blowing direction.-

Some idea of the potential of jets as a roll control can be derived from figure 17. Air obtained from simple scoop inlets was blown either normal to the fin surface from a row of orifices or in a spanwise direction from attached inlet stores. The normal blowing arrangement appears to be the most effective, although the store arrangement may be the most practical for some designs. The jet controls tested were not very efficient in comparison with deflected fins, but some gains are possible through increasing the size of the inlet or using an auxiliary high-energy source of gas. In the test case, the inlet and orifice areas were equal. The inlets occupied approximately 6 percent of the frontal area of the cruciform-fin model. The estimated thrust-force magnifications obtained with the jets blowing normal to the surface were about 10 at subsonic speeds and 3 at supersonic speeds.

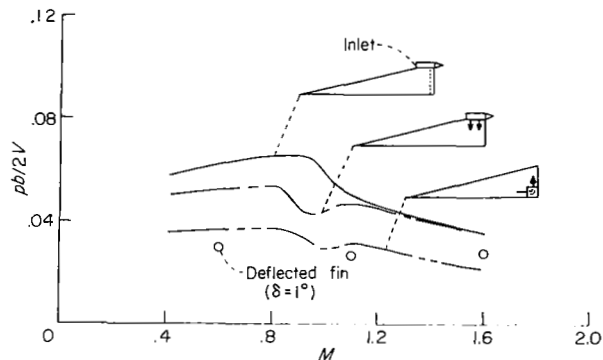


Figure 17.- Inlet-jet devices on 80° delta wings from reference 15.

#### CONCLUDING REMARKS

A rather brief summary of the pure roll performance of several control devices has been presented. The selection of any one control in preference to the others appears to be largely a matter of designer's choice, with some exceptions depending on the roll requirements in a given situation.

Langley Aeronautical Laboratory,  
National Advisory Committee for Aeronautics,  
Langley Field, Va., December 12, 1956.

## REFERENCES

1. Brewer, Jack D.: Description and Bibliography of NACA Research on Wing Controls. January 1946 - February 1955. NACA RM 54K24, 1955.
2. Strass, H. Kurt, Stephens, Emily W., Fields, E. M., and Schult, Eugene D.: Collection and Summary of Flap-Type-Aileron Rolling-Effectiveness Data at Zero Lift as Determined by Rocket-Powered Model Tests at Mach Numbers Between 0.6 and 1.6. NACA RM L55F14, 1955.
3. Nicolaidides, John D., and Bolz, Ray E.: On the Pure Rolling Motion of Winged and/or Finned Missiles in Varying Supersonic Flight. Jour. Aero. Sci., vol. 20, no. 3, Mar. 1953, pp. 160-168.
4. Adams, Gaynor J., and Dugan, Duane W.: Theoretical Damping in Roll and Rolling Moment Due to Differential Wing Incidence for Slender Cruciform Wings and Wing-Body Combinations. NACA Rep. 1088, 1952.
5. Tucker, Warren A., and Nelson, Robert L.: Theoretical Characteristics in Supersonic Flow of Constant-Chord Partial-Span Control Surfaces on Rectangular Wings Having Finite Thickness. NACA TN 1708, 1948.
6. Piland, Robert O.: Summary of the Theoretical Lift, Damping-in-Roll, and Center-of-Pressure Characteristics of Various Wing Plan Forms at Supersonic Speeds. NACA TN 1977, 1949.
7. Bland, William M., Jr.: Effect of Fuselage Interference on the Damping in Roll of Delta Wings of Aspect Ratio 4 in the Mach Number Range Between 0.6 and 1.6 as Determined With Rocket-Propelled Vehicles. NACA RM L52E13, 1952.
8. Graham, Ernest W.: A Limiting Case for Missile Rolling Moments. Jour. Aero. Sci., vol. 18, no. 9, Sept. 1951, pp. 624-628.
9. Stone, David G.: A Collection of Data for Zero-Lift Damping in Roll of Wing-Body Combinations as Determined With Rocket-Powered Models Equipped With Roll-Torque Nozzles. NACA TN 3955, 1957. (Supersedes NACA RM L53E26.)
10. Boissevain, Alfred G.: Experimental Investigation of the Damping in Roll of Cruciform Triangular Wing-Body Combinations at Mach Numbers From 1.5 to 6.0. NACA RM A54B15a, 1954.
11. Sandahl, Carl A., and Strass, H. Kurt: Comparative Tests of the Rolling Effectiveness of Constant-Chord, Full-Delta, and Half-Delta Ailerons on Delta Wings at Transonic and Supersonic Speeds. NACA RM L9J26, 1949.
12. Strass, H. Kurt: Summary of Some Rocket-Model Investigations of Effects of Wing Aspect Ratio and Thickness on Aileron Rolling Effectiveness Including Some Effects of Spanwise Aileron Locations for Sweptback Wings With Aspect Ratio of 8.0. NACA RM L53L11, 1953.

13. Fields, E. M., and Strass, H. Kurt: Free-Flight Measurements at Mach Numbers From 0.7 to 1.6 of Some Effects of Airfoil-Thickness Distribution and Trailing-Edge Angle on Aileron Rolling Effectiveness and Drag for Wings With  $0^\circ$  and  $45^\circ$  Sweepback. NACA RM L51G27, 1951.
14. Tucker, Warren A., and Nelson, Robert L.: Theoretical Characteristics in Supersonic Flow of Two Types of Control Surfaces on Triangular Wings. NACA Rep. 939, 1949. (Supersedes NACA TN's 1600 and 1601 by Tucker and TN 1660 by Tucker and Nelson.)
15. Schult, Eugene D.: Free-Flight Investigation at Mach Numbers Between 0.5 and 1.7 of the Zero-Lift Rolling Effectiveness and Drag of Various Surface, Spoiler, and Jet Controls on an  $80^\circ$  Delta-Wing Missile. NACA TN D-205, 1960. (Supersedes NACA RM L56H29.)
16. Tucker, Warren A., and Nelson, Robert L.: The Flexible Rectangular Wing in Roll at Supersonic Flight Speeds. NACA TN 1769, 1948.
17. Strass, H. Kurt: Additional Free-Flight Tests of the Rolling Effectiveness of Several Wing-Spoiler Arrangements at High Subsonic, Transonic, and Supersonic Speeds. NACA RM L81I23, 1948.
18. Schult, Eugene D., and Fields, E. M.: Free-Flight Measurements of the Rolling Effectiveness and Drag of Trailing-Edge Spoilers on a Tapered Sweptback Wing at Mach Numbers Between 0.6 and 1.4. NACA RM L53L14a, 1954.
19. Strass, H. Kurt, and Marley, Edward T.: Rolling Effectiveness of All-Movable Wings at Small Angles of Incidence at Mach Numbers From 0.6 to 1.6. NACA RM L51H03, 1951.
20. Bird, John D.: Some Theoretical Low-Speed Span Loading Characteristics of Swept Wings in Roll and Sideslip. NACA Rep. 969, 1950. (Supersedes NACA TN 1839.)
21. DeYoung, John: Spanwise Loading for Wings and Control Surfaces of Low Aspect Ratio. NACA TN 2011, 1950.
22. Lawrence, H. R.: The Lift Distribution on Low Aspect Ratio Wings at Subsonic Speeds. Jour. Aero. Sci., vol. 18, no. 10, Oct. 1951, pp. 683-695.
23. Tucker, Warren A., and Piland, Robert O.: Estimation of the Damping in Roll of Supersonic-Leading-Edge Wing-Body Combinations. NACA TN 2151, 1950.
24. Bland, William M., Jr., and Dietz, Albert E.: Some Effects of Fuselage Interference, Wing Interference, and Sweepback on the Damping in Roll of Untapered Wings as Determined by Techniques Employing Rocket-Propelled Vehicles. NACA RM L51D25, 1951.
25. Bleviss, Zegmund O.: Some Roll Characteristics of Cruciform Delta Wings at Supersonic Speeds. Jour. Aero. Sci., vol. 18, no. 5, May 1951, pp. 289-297.

26. Johnson, Harold S.: Wind-Tunnel Investigation at Low Transonic Speeds of the Effects of Number of Wings on the Lateral-Control Effectiveness of an RM-5 Test Vehicle. NACA RM L9H16, 1949.
27. Tucker, Warren A., and Nelson, Robert L.: The Effect of Torsional Flexibility on the Rolling Characteristics at Supersonic Speeds of Tapered Unswept Wings. NACA Rep. 972, 1950. (Supersedes NACA TN 1890.)
28. Strass, H. Kurt: Free-Flight Investigation of the Rolling Effectiveness at High Subsonic, Transonic, and Supersonic Speeds of Leading-Edge and Trailing-Edge Ailerons in Conjunction With Tapered and Untapered Plan Forms. NACA RM L8E10, 1948.
29. Sandahl, Carl A., Strass, H. Kurt, and Piland, Robert O.: The Rolling Effectiveness of Wing-Tip Ailerons as Determined by Rocket-Powered Test Vehicles and Linear Supersonic Theory. NACA RM L50F21, 1950.
30. Strass, H. Kurt, and Tucker, Warren A.: Some Effects of Aileron Span, Aileron Chord, and Wing Twist on Rolling Effectiveness as Determined by Rocket-Powered Model Tests and Theoretical Estimates. NACA RM L54G13, 1954.
31. Bobbitt, Percy J.: Linearized Lifting-Surface and Lifting-Line Evaluations of Sidewash Behind Rolling Triangular Wings at Supersonic Speeds. NACA Rep. 1301, 1957. (Supersedes NACA TN 3609.)
32. Strass, H. Kurt, and Stephens, Emily W.: An Engineering Method for the Determination of Aeroelastic Effects Upon the Rolling Effectiveness of Ailerons on Swept Wings. NACA RM L53H14, 1953.
33. Hedgepeth, John M., and Kell, Robert J.: Rolling Effectiveness and Aileron Reversal of Rectangular Wings at Supersonic Speeds. NACA TN 3067, 1954.
34. Hedgepeth, John M., Waner, Paul G., Jr., and Kell, Robert J.: A Simplified Method for Calculating Aeroelastic Effects on the Roll of Aircraft. NACA TN 3370, 1955.
35. Bland, William M., Jr.: Effect of Wing Flexibility on the Damping in Roll of a Notched Delta Wing-Body Combination Between Mach Numbers 0.6 and Approximately 2.2 as Determined With Rocket-Propelled Models. NACA RM L54E04, 1954.
36. Fields, E. M.: Some Effects of Spoiler Height, Wing Flexibility, and Wing Thickness on Rolling Effectiveness and Drag of Unswept Wings at Mach Numbers Between 0.4 and 1.7. NACA RM L52H18, 1952.
37. Holford, J. F., and Leathers, J. W.: Low Speed Tunnel Tests of Some Split Flap Arrangements on a  $48^\circ$  Delta Wing. Tech. Note No. Aero. 2188, British R.A.E., Sept. 1952.

38. Wiley, Harleth G.: A Wind-Tunnel Investigation at High Subsonic Speeds of the Lateral Control Characteristics of Various Plain Spoiler Configurations on a 3-Percent-Thick  $60^\circ$  Delta Wing. NACA RM L54D01, 1954.
39. Mueller, James N.: Investigation of Spoilers at a Mach Number of 1.93 to Determine the Effects of Height and Chordwise Location on the Section Aerodynamic Characteristics of a Two-Dimensional Wing. NACA TN 4180, 1958. (Supersedes NACA RM L52L31.)
40. Lord, Douglas R., and Czarnecki, K. R.: Pressure Distributions and Aerodynamic Characteristics of Several Spoiler-Type Controls on a Trapezoidal Wing at Mach Numbers of 1.61 and 2.01. NACA RM L56E22, 1956.
41. Franks, Ralph W.: The Application of a Simplified Lifting-Surface Theory to the Prediction of the Rolling Effectiveness of Plain Spoiler Ailerons at Subsonic Speeds. NACA RM A54H26a, 1954.
42. Schult, Eugene D., and Fields, E. M.: Free-Flight Measurements of Some Effects of Spoiler Span and Projection and Wing Flexibility on Rolling Effectiveness and Drag of Plain Spoilers on a Tapered Sweptback Wing at Mach Numbers Between 0.6 and 1.6. NACA RM L52H06a, 1952.
43. Purser, Paul E., and McKinney, Elizabeth G.: Comparison of Pitching Moments Produced by Plain Flaps and by Spoilers and Some Aerodynamic Characteristics of an NACA 23012 Airfoil With Various Types of Aileron. NACA WR L-124, 1945. (Formerly NACA ACR L5C24a.)
44. Vogler, Raymond D., and Turner, Thomas R.: Wind-Tunnel Investigation at Transonic Speeds of a Jet Control on a  $35^\circ$  Swept Wing - Transonic-Bump Method. NACA RM L55K09, 1956.
45. Turner, Thomas R., and Vogler, Raymond D.: Wind-Tunnel Investigation at Transonic Speeds of a Jet Control on an  $80^\circ$  Delta-Wing Missile. NACA RM L55H22, 1955.
46. English, Roland D.: Flight Investigation of an Aileron and a Spoiler on a Wing of the X-3 Airplane Plan Form at Mach Numbers From 0.5 to 1.6. NACA RM L54D26a, 1954.
47. Purser, Paul E., and Stevens, Joseph E.: Exploratory Rocket Flight Tests to Investigate the Use of a Freely Spinning Monoplane Tail for Stabilizing a Body. NACA RM L52I05a, 1952.
48. Nelson, Robert L.: The Motions of Rolling Symmetrical Missiles Referred to a Body-Axis System. NACA TN 3737, 1956.
49. Toll, Thomas A., and Queijo, M. J.: Approximate Relations and Charts for Low-Speed Stability Derivatives of Swept Wings. NACA TN 1581, 1948.
50. Chubb, Robert S.: Experimental Investigation of the Static Aerodynamic and Dynamic Damping-in-Roll Characteristics of an 8-CM Aircraft Rocket With Solid and Slotted Fins. NACA RM A52C04, 1952.

51. Schult, Eugene D.: A Free-Flight Investigation at High Subsonic and Low Supersonic Speeds of the Rolling Effectiveness and Drag of Three Spoiler Controls Having Potentially Low Actuating-Force Requirements. NACA RM L55G11a, 1955.